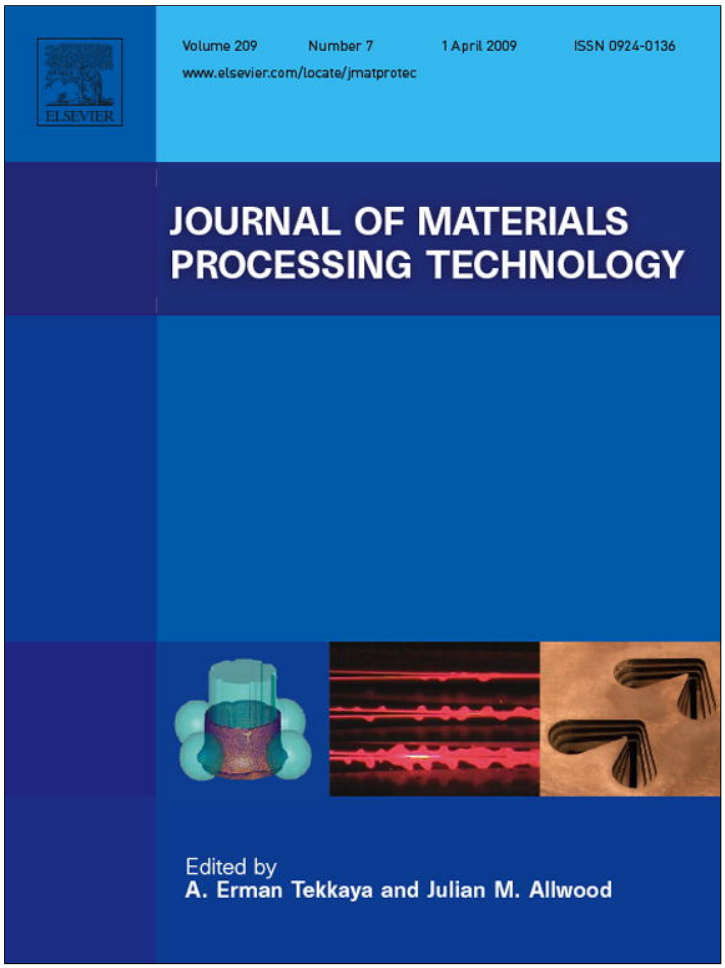

JOURNAL OF MATERIALS PROCESSING TECHNOLOGY 209 (2009) 3650–3656

journal homepage: www.elsevier.com/locate/jmatprotec

Kinematics of metal flow during twist extrusion investigated with a new experimental method

Y. Beygelzimer, A. Reshetov, S. Synkov, O. Prokof'eva, R. Kulagin*

Donetsk Physics & Engineering Institute of the National Academy of Sciences of Ukraine, Department of High Pressure Physics and Advanced Technologies, 72 R. Luxemburg Street, Donetsk 83114, Ukraine

ARTICLE INFO

Article history:
Received 23 April 2008
Received in revised form
13 August 2008
Accepted 27 August 2008

Keywords:
Twist extrusion
Strain distribution
Experimentally kinematic method

ABSTRACT

We propose an experimental method for investigating the kinematics of metal flow in twist extrusion (TE). The method is based on a theoretical model of the velocity field. The parameters of this model are determined to satisfy the observed flow-line for characteristic points of the specimen. The model incorporates two physical constraints: (1) metal flow is limited by the surface of the die; (2) metal volume remains constant. The advantage of this method is that it takes into account the actual rheology of the metal and friction conditions.

We show that TE forms a vortex-like flow that stretches metal particles. The stretching increases with subsequent TE passes. The equivalent strain increases from 0.3 to 0.5 in the paraxial zone of the specimen to 2.0–2.5 at the periphery.

We analyze different sources of inaccuracy of the method and show that its error in estimating the equivalent strain is of the order of 0.1, which is perfectly acceptable when investigating severe plastic deformations.

1. Introduction

Twist extrusion (TE) is a severe plastic deformation (SPD) process. SPD processes use extensive hydrostatic pressure to impose very high strain on bulk solids, producing exceptional grain refinement without introducing any significant change in the overall dimensions of the sample (Valiev et al., 2006).

The two most widely used SPD methods are high-pressure torsion (HPT) (Smirnova et al., 1986) and equal-channel angular pressing (ECAP) (Segal et al., 1981). The advantage of HPT over ECAP is that it tends to produce both smaller grain sizes and a higher fraction of boundaries with high-angle misorientations (Sakai et al., 2005). A major disadvantage of HPT, however, is a small specimen size. Several SPD schemes were proposed to deal with this problem. These schemes can realize torsion under pressure in sufficiently large specimens. The work of Sakai et al. (2005) demonstrates the feasibility of extending HPT to cylindrical specimens that are significantly larger than the conventional thin disks but are still far smaller than ECAP specimens. The problem was completely resolved with the introduction of SPD processes that combine extrusion with torsion. In TE (Beygelzimer et al., 2002), twisting of the specimen occurs due to the special form of the extrusion die. In torsion extrusion (Mizunuma, 2006) and shear extrusion method (Segal, 2006), it is realized by twisting the die around the container. In principle, the later solution can allow for a larger accumulation of equivalent strain in one pass, significantly larger than achievable with TE. In obtaining submicrocrystalline (SMC) materials, however, this is not always reasonable since it can lead to a significant heating of specimens and recrystallization of the metal. It is also important to take into account that TE is done using standard pressure equipment, while processes based on twisting the die require additional equipment and energy sources.

* *Corresponding author*. Tel.: +380 62 311 5273; fax: +380 62 337 7608.
E-mail address: yanbeygel@gmail.com (Y. Beygelzimer).
0924-0136/$ – see front matter © 2008 Elsevier B.V. All rights reserved.
doi:10.1016/j.jmatprotec.2008.08.022

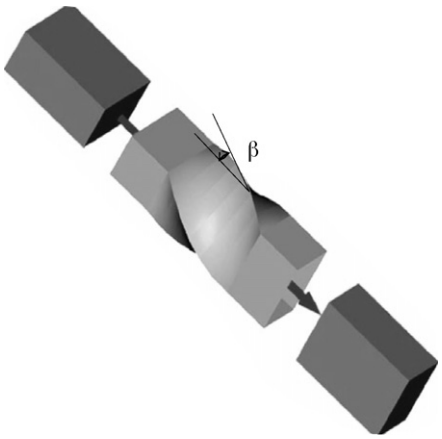

Fig. 1 – Twist extrusion scheme.

TE was proposed by the first author in Beygelzimer et al. (1999). The basic idea is to press out a prism specimen through a die with a profile consisting of two prism sections separated by a twist section (see Fig. 1). As the specimen is processed, it undergoes severe deformation while maintaining its original cross-section. This property allows the specimen to be extruded repeatedly in order to accumulate strain, allowing one to control the structure and properties of the specimen.

The kinematics of metal flow during TE is substantially different from that of other SPD processes (e.g., ECAP, HPT, torsion extrusion, shear extrusion method), which opens possibilities for investigating and forming new structures with new properties. For this reason, investigating the kinematics of TE is of significant interest.

A first approximation of the kinematics was obtained by a variational method in (Beygelzimer et al., 2002). Mousavi et al. (2007) and Yoon et al. (2006) analyzed the strain–stress distribution using the finite element method (FEM).

However, there are several reasons why it is important to perform experimental studies of the kinematics of TE as well. The problem of large plastic deformation during TE is highly nonlinear. This nonlinearity is due to the resistance of the material to external stress (physical nonlinearity), and also due to finite displacements of material particles (geometrical nonlinearity). Both sources of nonlinearity lead to errors in numerical calculations. In particular, the universal strain–stress curve and the von Mises theory of plasticity, which form the basis of most calculations, rely on assumptions that are often too strong in practice. A crucial observation is that metal rheology determined in test experiments may be noticeably different from the rheology during complex loading. This observation is especially relevant for TE since TE realizes complex loading that includes elements of simple and pure shear, and it is well known that stress–strain curves of many metals are significantly different in these tests (see, for example, Bridgman, 1952).

In addition, the problem of estimating the friction during TE is complicated by the unknown rheology and by a significant non-monotone change of the specimen surface area during TE.

The errors due to geometrical nonlinearity are often discussed in FEM studies (Sadakov and Shapiro, 2003; Wagoner and Chenot, 2001). The magnitude of these errors depends on a particular task; for large shear, as in TE, the error can become unacceptable. These factors make it important to complement numerical analysis with experimental methods, which do not rely on assumptions made by numerical methods.

This paper proposes one such method and uses it to analyze the kinematics of metal flow during TE.

2. Proposed method for experimental estimation of TE kinematics

2.1. Main idea

The basic idea is to reconstruct metal flow during TE using experimental stream-lines. We start with a specimen with nine fibers embedded along its main axis. The specimen is pressed through a built-up twist die until the stationary flow is reached. The specimen is then removed from the die and cut perpendicularly to its main axis, at small intervals. In each cross-section, we measure the coordinates of the markers (fiber cuts).

To approximate experimental stream-lines, we use a class of kinematically admissible velocity fields (KAVF). The class is determined by two natural conditions: (1) metal volume remains constant (incompressibility condition), and (2) metal flow is limited by the surface of the die (impenetrability condition). The KAVF is chosen to be the closest match to the experimentally obtained stream-line data. The resulting velocity field is then used to find the strain state of the metal using relations of continuum mechanics.

2.2. Theoretical model for kinematically admissible velocity fields

According to a well-known theorem in vector analysis (Marsden and Tromba, 2003), every vector field $\vec{V}$ that satisfies the incompressibility condition, can be represented as

$$\vec{V} = \mathrm{rot}\,\vec{A}, \tag{1}$$

where $\vec{A}$ is the vector potential.

Beygelzimer and Palant (1981) show that for an arbitrary channel, any KAVF can be obtained from the following universal expression for the vector potential:

$$\vec{A} = \vec{A}_0 + \varpi\vec{P} \tag{2}$$

where $\vec{A}_0$ is the vector field for which (1) satisfies boundary conditions imposed on the velocity field; ϖ is the so called shape function of the channel that satisfies the following conditions: $\varpi = 0$ on the channel surface, $\varpi > 0$ inside the channel, and $\varpi < 0$ otherwise; $\vec{P}$ defines the varying part of the velocity field and is an arbitrary field satisfying the smoothness condition. Rvachev developed the method for determining shape functions for arbitrary geometric forms (see, for example, (Rvachev et al., 1994)).

The first term in (2) specifies a particular KAVF satisfying given boundary conditions on $\vec{V}$ given in (1), while the second

term gives a general expression for KAVF with zero velocity on the boundary.

It is easy to show that the velocity field (1) given by $\vec{A} = \varpi\vec{P}$ determines a flow limited by the surface of the die. Indeed, the impenetrability condition has the following form:

$$V_n = \vec{n}\vec{V} = 0, \tag{3}$$

where $\vec{n}$ is the normal vector to the channel's surface.

It is well-known (Marsden and Tromba, 2003) that

$$\vec{n} = \text{grad}\ \varpi \tag{4}$$

We can determine V_n using the expression $\vec{V} = \text{rot}(\varpi\vec{P})$:

$$\begin{aligned} V_n = \vec{n}\vec{V} &= \text{grad}\ \varpi \cdot \text{rot}(\varpi\vec{P}) = \text{grad}\,\varpi \cdot (\varpi\,\text{rot}\,\vec{P} + \text{grad}\,\varpi \times \vec{P}) \\ &= \varpi\,\text{grad}\,\varpi \cdot \text{rot}\,\vec{P} + \text{grad}\,\varpi \cdot (\text{grad}\,\varpi \times \vec{P}) \end{aligned} \tag{5}$$

The first term in expression (5) is zero on the channel's surface since $\varpi = 0$ on the surface. The second term is identically zero (Marsden and Tromba, 2003). Therefore, the second term of the velocity field satisfies the impermeability condition.

Let $\vec{A}_0$ be defined as following:

$$A_{0x} = 0.5V_0 y, \quad A_{0y} = -0.5V_0 x, \quad A_{0z} = -\frac{V_0\ \tan\beta}{R}xy \tag{6}$$

where V_0 is the extrusion speed; R is the radius of the circle around the cross-section of the die channel; and β corresponding to R is the angle between the twist line and the extrusion axis (see Fig. 1).

Relation (6) assumes that β changes from top to bottom of the die, i.e., $\beta = \beta(z)$, so that $\beta = 0$ in prismatic regions, while $\beta > 0$ in the twist region.

The vector potential (6) implies the following field $\vec{V}$:

$$V_{1x} = -\frac{yV_0\ \tan\beta}{R}, \quad V_{1y} = \frac{xV_0\ \tan\beta}{R}, \quad V_{1z} = -V_0 \tag{7}$$

which describes the "twist flow" of the metal, i.e., the motion of the entire cross-section along the twist channel. It is easy to see that this partial velocity field defines a flow limited by the surface of the die and satisfies conjugation conditions at rigid ends of the specimen.

Let vector $\vec{P}$ be in the following form:

$$P_x = 0, \quad P_y = 0, \quad P_z = P(z), \tag{8}$$

which leads to the following varying part $\vec{V}_2 = \text{rot}(\omega\vec{P})$ of the velocity field:

$$V_{2x} = P(z)\frac{\partial\varpi}{\partial y}, \quad V_{2y} = -P(z)\frac{\partial\varpi}{\partial x}, \quad V_{2z} = 0 \tag{9}$$

According to (9), we assume that $\vec{V}_2$ defines metal flow-over within the cross-section of the specimen and does not influence the flow velocity in the direction of extrusion, which, according to (7), satisfies $V_{1z} = -V_0$ in the entire cross-section. We will justify this assumption below.

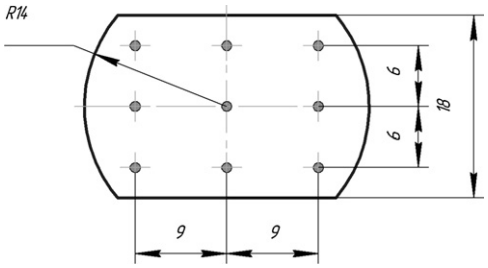

Fig. 2 – A cross-section of the billet in TE. The figure shows the position of the fibers in the cross-section.

According to the velocity field (7) and (9), components of the strain velocity tensor can be calculated from

$$\begin{aligned} &\dot{\varepsilon}_{xx} = P\frac{\partial^2\omega}{\partial x\partial y}, \quad \dot{\varepsilon}_{yy} = -P\frac{\partial^2\omega}{\partial x\partial y}, \quad \dot{\varepsilon}_{xy} = \frac{1}{2}P\left(\frac{\partial^2\omega}{\partial y^2} - \frac{\partial^2\omega}{\partial x^2}\right), \\ &\dot{\varepsilon}_{xz} = \frac{1}{2}\frac{\partial^2(\omega P)}{\partial y\partial z} - \frac{yV_0}{2R\ \cos^2\beta}\frac{d\beta}{dz}, \\ &\dot{\varepsilon}_{yz} = -\frac{1}{2}\frac{\partial^2(\omega P)}{\partial x\partial z} + \frac{xV_0}{2R\ \cos^2\beta}\frac{d\beta}{dz}. \end{aligned} \tag{10}$$

The strain rate $\dot{\varepsilon}_i$ and the von Mises equivalent strain e are determined using the following formulas:

$$\dot{\varepsilon}_i = \frac{\sqrt{2}}{3}\sqrt{(\dot{\varepsilon}_{xx}-\dot{\varepsilon}_{yy})^2+(\dot{\varepsilon}_{xx}-\dot{\varepsilon}_{zz})^2+(\dot{\varepsilon}_{zz}-\dot{\varepsilon}_{yy})^2+6(\dot{\varepsilon}_{xy}^2+\dot{\varepsilon}_{xz}^2+\dot{\varepsilon}_{yz}^2)}, \tag{11}$$

$$e = \int \varepsilon_i\ dt. \tag{12}$$

3. Example of the method in use

We performed experiments using copper prism-shaped specimens of length 60 mm, with the cross-section as in Fig. 2. Nine aluminum fibers, with diameter 1.00 ± 0.05 mm and length 50 mm, were embedded along the main axis of the specimen. Fig. 2 shows the position of the fibers in the cross-section. For TE, we used a built-up twist die with dependence $\beta(z)$ given in Fig. 3. TE was performed at room temperature (298 K) under constant backpressure of 200 MPa. Each specimen was extruded until the stationary flow was reached, and was then removed from the die. We cut the front non-stationary end

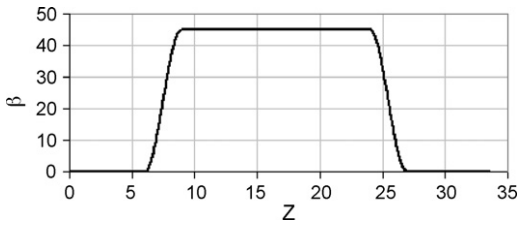

Fig. 3 – The plot shows how the inclination angle β depends on the axial coordinate.

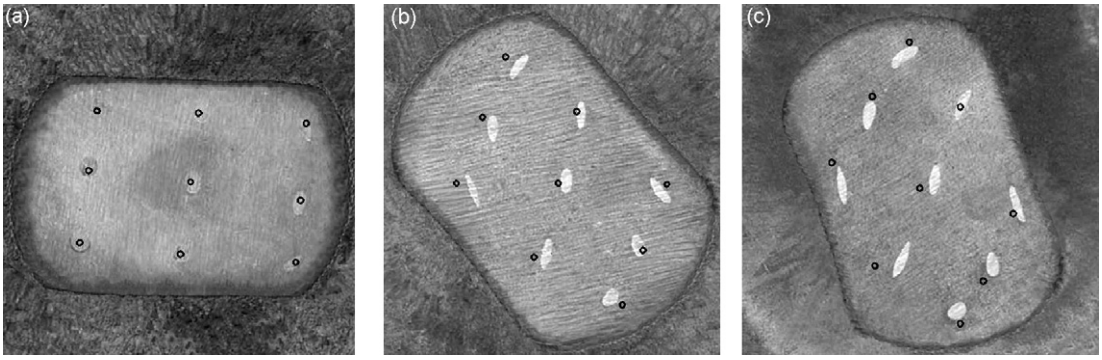

Fig. 4 – Billet's cross-sections with fibers markers: (a) cross-section #6, (b) cross-section #17 and (c) cross-section #24. Black circles mark theoretical streamlines.

(of length roughly 10 mm) and then shaved the specimen perpendicularly to its main axis with an interval of 1.0 mm. This process successively gave 35 cross-sections. The face-plate of each cross-section was etched in 50% nitric acid solution to reveal the markers. The plate was then digitized with a scanner. The markers were approximated by ellipses whose centers were taken to be the traces of the experimental stream-lines. Fig. 4 illustrates three cross-sections with the markers.

According to Rvachev et al. (1994), the shape function ϖ of the twist channel with the cross-section in Fig. 2, has the following form:

$$\varpi = \Omega_1 + \Omega_2 - \sqrt{\Omega_1^2 + \Omega_2^2} \tag{13}$$

where $\Omega_1 = 1/2R(R^2 - \xi^2 - \eta^2)$, $\Omega_2 = 1/h((0,5h)^2 - \eta^2)$. Here R and h are the dimensions of the die cross-section in Fig. 2 ($R = 14$ mm, $h = 18$ mm), and

$$\begin{cases} \xi = x\cos\varphi(z) + y\sin\varphi(z) \\ \eta = -x\sin\varphi(z) + y\cos\varphi(z) \end{cases}, \tag{14}$$

where $\varphi(z) = (z/R)\tan\beta(z)$ is a rotation angle of the cross-section contour as a function of z.

The function $P(z)$ is found by minimizing the disparity between experimental stream-lines and theoretical stream-lines obtained by means of $\tilde{V}$ in (7) and (9). Disparity is determined using the following expression:

$$r = \max\frac{\rho_{ik}}{R}, \quad i = 1, \ldots, 9, \quad k = 1, \ldots, 35 \tag{15}$$

where ρ_{ik} is the error in predicting the i-th streamline in the k-th cross-section; R is the radius of the circle around the cross-section.

Our experience with using the method showed that for twist dies with an almost rectangular cross-section (see Fig. 2), good approximations of the experimental stream-lines give the following expression for $P(z)$ with only one parameter:

$$P(z) = C\beta(z) \tag{16}$$

Fig. 5 shows the relationship between r and C for the described experiment. The relation shows the presence of a fairly pronounced extreme in point $C^* = -1.07$. The corresponding value of disparity is $r^* = 0.11$. The next section estimates the inaccuracy of TE kinematics due to this disparity.

Fig. 6 shows the velocity field in the cross-section, in the center of the twist region of the die. It is clear that TE forms a vortex-like flow. Such a flow stretches metal particles, and the stretching increases with subsequent TE passes. This phenomenon is illustrated by Fig. 7, which shows the distortion of the shape of the particles after one and seven TE passes, respectively.

Fig. 8 shows how the equivalent strain depends on the coordinate along the extrusion axis.

Fig. 9 illustrates the accumulated strain distribution within the billet cross-section.

Despite the inhomogeneity of deformation, the structure and properties of materials tend to even out with subsequent TE passes. This is due to stabilization of structure and saturation of properties after the strain exceeds some saturation levels (Beygelzimer et al., 2006). Such stabilization and saturation are not unique to TE. They are typically present in any deformation method based on simple shear. For example, saturation occurs in ECAP (Valiev and Langdon, 2006) and torsion (Bridgman, 1952). A possible mechanism explaining this effect in SPD is analyzed in (Beygelzimer, 2005). As the number of passes increases, the zone where strain exceeds

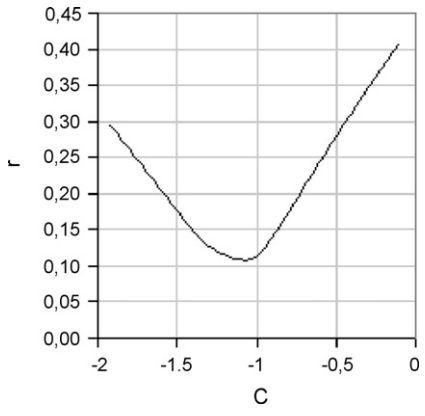

Fig. 5 – The plot shows how disparity r depends on parameter C.

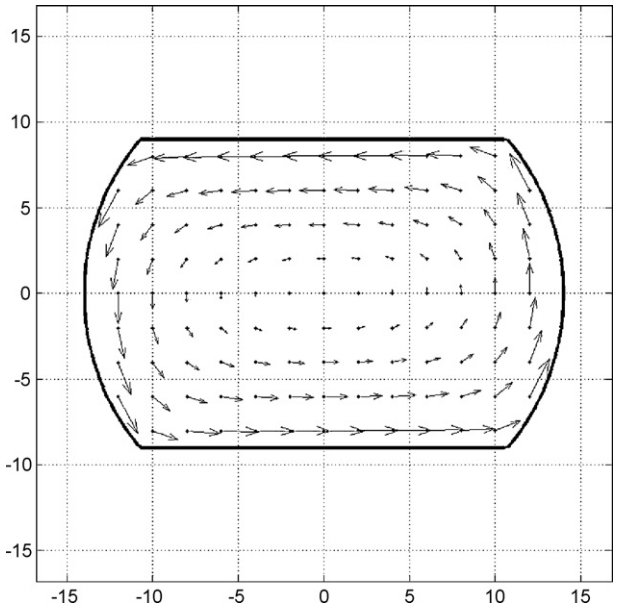

Fig. 6 – Velocity field in a cross-section, in the center of the die's twist region.

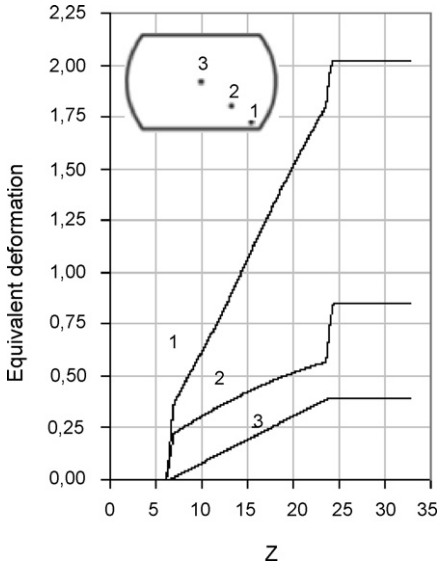

Fig. 8 – Equivalent strain versus coordinate along the extrusion axis (*Z*) for representative points of the specimen cross-section.

the saturation threshold, gradually fills up the entire cross-section. This tends to level out the structure and properties across the billet's cross-section (Beygelzimer et al., 2006; Orlov et al., 2008).

4. Estimating the inaccuracy of the method

The kinematics of an incompressible medium's stationary flow is completely determined by stream-lines (Milne-Thomson, 1960), so the inaccuracies in the method come from the inaccuracies in determining the stream-lines.

First, note that there is an unremovable error due to the finite sizes of the fibers' cross cuts. The fibers represent fluid tubes, whose round cross-sections are distorted as we move along the extrusion axis (see Fig. 4). This distortion leads to some unavoidable uncertainty in the location of the experimental stream-lines. We approximated fiber cross-cuts by ellipses whose centers were taken to be the traces of the actual stream-lines. The inaccuracy due to this assumption is of the order of deciles of the actual cross-cut sizes, which is significantly less than the disparity r due to approximating experimental stream-lines with theoretical stream-lines. For this reason, we consider only the disparity r.

Let us estimate the error of the method due to r using some kinematic characteristic χ. For this purpose, we determine the sensitivity of χ to r, i.e., the value of $\partial\chi/\partial r$. The absolute error of the method in estimating χ can be determined as

$$\Delta\chi = \frac{\partial\chi}{\partial r} r_{\mathrm{exp}}, \tag{17}$$

where r_{exp} is the empirical value of r.

If the space of KAVFs contained the true field, then the value of $\partial\chi/\partial r$ could be estimated numerically by perturbing the coordinates of the markers around their empirical values. However, we assumed that $V_z = V_0 = \mathrm{const}$, and first we need to estimate the error due to this assumption.

The condition of volume invariability implies the following relation of metal flows in the 0-th and k-th cross-sections of

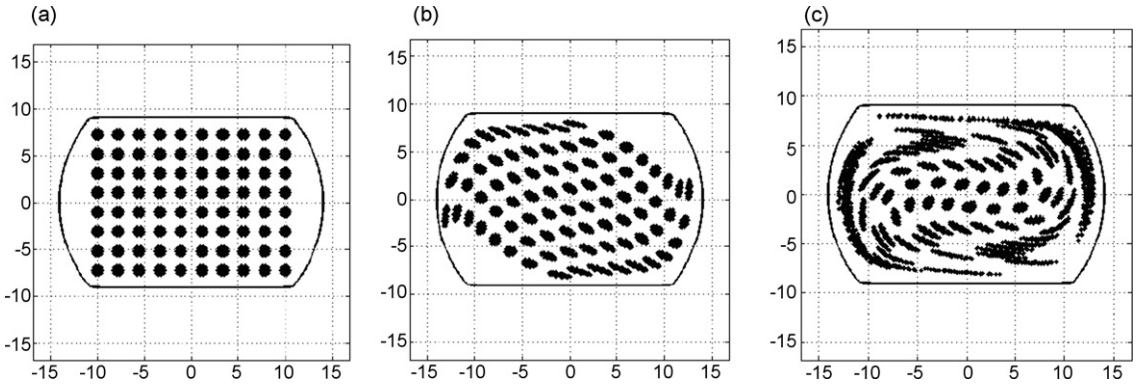

Fig. 7 – Shape distortion of metal particles (a) after a single pass of TE (b), and seven passes (c).

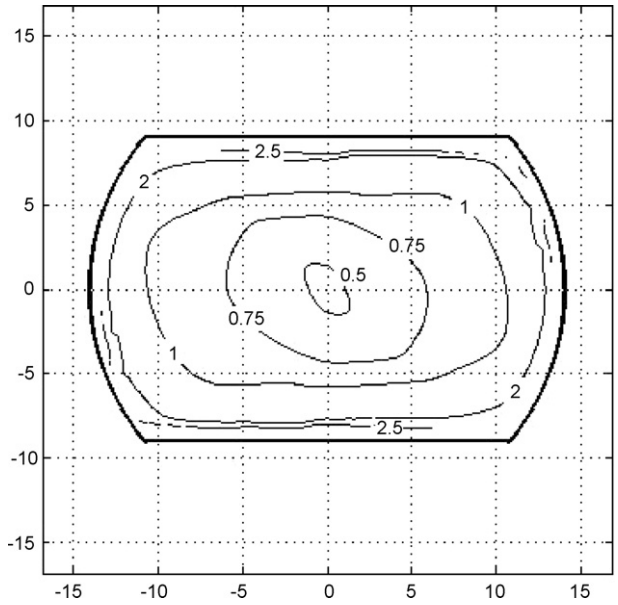

Fig. 9 – Distribution of equivalent strain within the billet cross-section after one pass of TE.

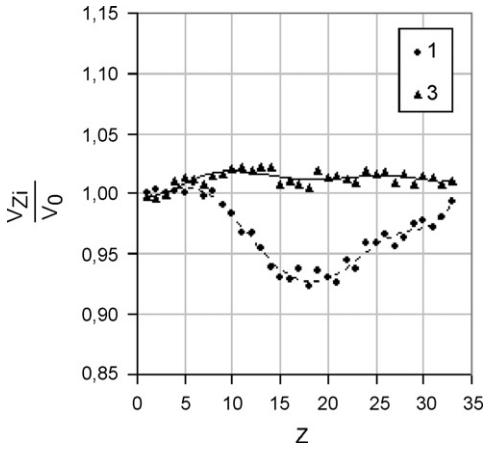

Fig. 10 – The value of V_{zk}/V_0 for the stream-lines that are furthest (1) and closest (3) to the specimen axis (1, 3 correspond to the Fig. 8).

the specimen:

$$\bar{V}_{zk}S_k = V_0S_0 \tag{18}$$

where $\bar{V}_{zk}$ is the average value (across the cross-section) of the axial component of the velocity, S_0 and S_k are the areas of the 0-th and k-th cross-sections, respectively.

The method we use to produce twist dies guarantees, with high precision, the consistency of the cross-section along the height. The backpressure ensures that the metal nearly completely fills up the die during TE. Measuring cross-section areas of a specimen stopped in a twist die shows that the difference between S_k and S_0 does not exceed 3%. This implies that $\bar{V}_{zk}$ differs from V_0 by no more than 3%.

Local values of V_{zk} for experimental stream-lines can be estimated from the following formula, which follows from the condition that the fiber volume remains constant:

$$V_{zk} = V_0\frac{s_0}{s_k}. \tag{19}$$

Here s_0 and s_k are fiber cross-cut areas before the deformation and in the k-th cross-section, respectively.

Experiments show that the largest deviation of V_z from V_0 is observed for the stream-lines furthest from the specimen axis. Also, V_z is smaller on the periphery than on the axis, which leads to a warping effect. Fig. 10 gives V_{zk}/V_0 for the stream-lines that are furthest and closest to the specimen axis.

According to Fig. 10, the inaccuracy in the velocity under the assumption $V_z = V_0 = \text{const}$, does not exceed 10%.

Assuming $V_z = \text{const}$, we essentially ignore the derivatives of this component of the velocity. Doing so leads to the following error in estimating the strain rate $\dot{\varepsilon}_i$:

$$\delta = \frac{|\dot{\varepsilon}'_i - \dot{\varepsilon}_i|}{\dot{\varepsilon}_i} \tag{20}$$

where $\dot{\varepsilon}_i$ and $\dot{\varepsilon}'_i$ are the strain rates with and without taking into account the derivatives of V_z (respectively).

For computing δ, the derivatives $\partial V_z/\partial z$ were determined via numerical differentiation of functions V_z specified in the 35 cross-sections (see Fig. 10), and for $\partial V_z/\partial x$ and $\partial V_z/\partial y$, we used the estimates $|\partial V_z/\partial x| \sim |\partial V_z/\partial y| \sim |V_z - V_0/R|$. The largest value of δ is reached at the peripheral stream-lines, where δ does not exceed 0.10. This way, the error in estimating the strain rate under the assumption $V_z = V_0 = \text{const}$, does not exceed 10%. Clearly, this assumption leads to an error of the same order in estimating the von Mises equivalent strain.

Finally, we analyze the error in estimating the equivalent strain, which comes from the error r in approximating experimental stream-lines by the adopted class of KAVFs. To estimate this error, we performed a numerical experiment consisting of randomly perturbing the position of "experimental" stream-lines inside the tubes surrounding the actual experimental stream-lines. The diameter of these tubes was three times the diameter of the original fiber. For each new position of the markers, we minimized the disparity r, computed C^*, r^* and the equivalent strain for the nine stream-lines in the last cross-section of the specimen (with the full accumulated strain). Then we plotted the dependencies $e_k = e_k(r^*)$ (where $k = 1, \ldots, 9$ indexes the stream-line) and determined the sensitivities $\partial e_k/\partial r^*$. The experiment showed that the maximum sensitivity is $(\partial e_k/\partial r^*)_{\max} = 0.80$, reached for the stream-line that is furthest from the axis. From (12), using the experimentally obtained value of $r^* = 0.11$, we get the following estimate of the error in approximating the equivalent strain: $\Delta e = 0.09$.

5. Conclusions

The previous section shows that the proposed experimental method for investigating the kinematics of plastic flow in twist extrusion gives sufficiently accurate estimates of stream-lines, velocity field and equivalent strain.

The advantage of this method is that it takes into account the actual rheology of the metal and friction conditions. Thus

values obtained using this method, in particular the coordinates of stream-lines, can be used for studying the adequacy of solutions obtained using numerical methods.

Based on the proposed method, we show that twist extrusion forms a vortex-like flow that stretches metal particles. The stretching increases with subsequent passes. The full accumulated strain increases from 0.3–0.5 in the paraxial zone of the specimen to 2.0–2.5 at the periphery.

REFERENCES

Beygelzimer, Y., 2005. Grain refinement versus voids accumulation during severe plastic deformations of polycrystals: mathematical simulation. Mech. Mater. 37 (7), 753–767.

Beygelzimer, Y., Palant, Y., 1981. Structure of the solenoidal velocity field for the hydroextrusion problem. Math. Phys. 31, 66–67 [in Russian].

Beygelzimer, Y., Varyukhin, V.N., Synkov, S.G., Sapronov, A.N., Synkov, V.G., 1999. New schemes of large plastic deformations accumulating with using of hydroextrusion. Phys. Technol. High Press. 9 (3), 109–111 [in Russian].

Beygelzimer, Y., Orlov, D., Varyukhin, V., Sapronov, A.N., Synkov, V.G., 2002. A new severe plastic deformation method: twist extrusion. In: Zhu, Y.T., Langdon, T.G., Mishra, R.S., Semiatin, S.L., Saran, M.J., Lowe, T.C. (Eds.), Proceedings of Ultrafine Grained Materials II, TMS 2002 (The Minerals, Metals & Materials Society) Annual Meeting. Warrendale, PA, USA, pp. 297–304.

Beygelzimer, Y., Orlov, D., Korshunov, A., Synkov, S., Varyukhin, V., Vedernikova, I., Reshetov, A., Synkov, A., Polyakov, L., Korotchenkova, I., 2006. Features of twist extrusion: method, structures & material properties. Solid State Phenom. 114, 69–78.

Bridgman, P., 1952. Studies in Large Plastic and Fracture. McGraw-Hill, New York, 444 p.

Marsden, J.E., Tromba, A.J., 2003. Vector Calculus, 5th ed. W.H. Freeman & Co., New York, 704 p.

Milne-Thomson, L.M., 1960. Theoretical Hydrodynamics, 4th ed. MacMillan & Co. LTD., London, 660 p.

Mizunuma, S., 2006. Large straining behaviour and microstructure refinement of several metals by torsion extrusion process. Mater. Sci. Forum 503/504, 185–190.

Mousavi, A.A., Shahab, A.R., Mastoori, M., 2007. Three dimensional numerical analysis of twist extrusion process for annealed copper. Phys. Technol. High Press. 17 (1), 18–23.

Orlov, D., Beygelzimer, Y., Synkov, S., Varyukhin, V., Horita, Z., 2008. Evolution of microstructure and hardness in pure Al by twist extrusion. Mater. Trans. 49 (1), 2–6.

Rvachev, V.L., Shevchenko, A.N., Tsukanov, I.G., 1994. Application of R-function to the construction of realistic images. Pattern Recognit. Image Anal. 4 (2), 123–134.

Sadakov, O.S., Shapiro, A.A., 2003. About solution correctness of geometrically nonlinear problems with FEM package. Trans. South-Ural State Univ. (Math. Phys. Chem. Ser.) 3 (6), 21–23 [in Russian].

Sakai, G., Nakamura, K., Horita, Z., Langdon, T.G., 2005. Developing high-pressure torsion for use with bulk samples. Mater. Sci. Eng. A 406, 268–273.

Segal, V., 2006. Shear Extrusion Method. United States Patent US 7,096,705 B2.

Segal, V.M., Reznikov, V.I., Drobyshevskiy, A.E., Kopylov, V.I., 1981. Plastic working of metals by simple shear. Metals 1, 99–105 (in Russian).

Smirnova, N.A., Levit, V.I., Pilyugin, V.I., Kuznetsov, R.I., Davydova, L.S., Sazonova, V.A., 1986. Evolution of the structure of f.c.c. single crystal subjected to strong plastic deformation. Fiz. Met. Metalloved. 61, 1170–1177.

Valiev, R.Z., Langdon, T.G., 2006. Principles of equal-channel angular pressing as processing tool for grain refinement. Progr. Mater. Sci. 51, 881–981.

Valiev, R.Z., Estrin, Y., Horita, Z., Langdon, T.G., Zehetbauer, M.J., Zhu, Y.T., 2006. Producing bulk ultrafine-grained materials by severe plastic deformation. JOM 58 (4), 33–39.

Wagoner, R.H., Chenot, J.-L., 2001. Metal Forming Analysis. Cambridge University Press, New York, 368 p.

Yoon, S.C., Jang, Y.S., Kim, H.S., 2006. Plastic deformation of metallic materials during twist extrusion processing. J. Kor. Inst. Met. Mater. 44 (7), 480–484.